American Journal of Vehicle Design, 2014, Vol. 2, No. 1, 22-31
Available online at http://pubs.sciepub.com/ajvd/2/1/4

DOI:10.12691/ajvd-2-1-4

Numerical Assessment and Shape Optimization of Dissipative Muffler and Its Effect on I.C. Engine Acoustic Performance

Sabry Allam*

Automotive Technology Department, Faculty of Industrial Education, Helwan University, Cairo, Egypt
*Corresponding author: allam@kth.se

Received October 27, 2014; Revised November 22, 2014; Accepted November 27, 2014

Abstract Passive mufflers are widely employed to reduce industrial and domestic ventilation noise as well as vehicle exhaust noise. Their basic geometry is formed by a simple expansion chamber and the performance is controlled by using complex geometries or by adding porous materials inside the chamber. However, when a clean absorbent system is desirable or when the muffler must support high air flux, it is not possible to add those fibrous materials and the use of micro perforated panels (MPP) as another alternative to improve the acoustic performance become important. The purpose of this work is not only to optimize the acoustic performance of low cost simple geometry mufflers using MPP but also to find the best shape design under a limited space constraint aiming at improving the acoustic performance of automotive engines. In this paper, on the basis of plane wave theory, the four-port system matrix for two wave guides coupled via a MPP tube is derived and used to compute the two-port transfer matrix for an expansion chamber muffler with a MPP tube. Two different procedures to optimize the muffler acoustic performance; the acoustical based and the numerical based methods are presented under the same boundary conditions at a targeted frequency of 1500 Hz. Different methods to improve the MPP wall impedance are presented and compared. New optimized muffler is proposed and used to study the acoustic performance of four-cylinder diesel engine and compared with its performance using the existing straight through resonator muffler. It has been shown that the new optimized muffler reduces the engine noise around 6 dB(A), and also reduces the brake specific fuel consumption of the same engine about 8 percent at same operating conditions.

Keywords: *MPP, numerical assessment, dissipative muffler, shape optimization, engine noise, pressure drop, fuel consumption*

Cite This Article: Sabry Allam, "Numerical Assessment and Shape Optimization of Dissipative Muffler and Its Effect on I.C. Engine Acoustic Performance." *American Journal of Vehicle Design*, vol. 2, no. 1 (2014): 22-31. doi: 10.12691/ajvd-2-1-4.

1. Introduction

1.1. Background

Automobiles are nowadays one of the major sources of noise pollution and, when attention is focused on urban areas, automobiles appear to be the largest source. It is common experience that trucks are one of the noisiest vehicles on the road. This is primarily due to their low power/weight ratio, which requires them to operate almost at full power during acceleration and steady state operation. Moreover, for the same power rating, diesel engines are noisier than gasoline engines, since the combustion characteristics of diesel engines produce more harmonics than the slower combustion of gasoline. An unmuffled gasoline engine radiates exhaust noise in the range from 90 to 100 dB(A), while an unmuffled diesel engine under identical conditions radiates exhaust noise in the range from 100 to 125 dB(A) [1,2,3].

Measurements of the exhaust pipe pressure pulse on a IC engine [4] show that the majority of the pulse energy lies in the frequency range of 0-600 Hz. Exhaust mufflers are designed to reduce sound levels at these frequencies.

Industrial flow ducts as well as internal combustion engines frequently make use of silencing elements to attenuate the noise levels carried by the fluids and radiated to the outside atmosphere by the exhausts. Design of a complete muffler system is usually, a very complex task because each of its elements is selected by considering its particular acoustic performance and its interaction effects on the entire acoustic system performance [1,2,3].

Mufflers are conventionally classified as either passive or active type. Passive mufflers fall into two categories: dissipative or reactive, depending on whether the acoustic energy is dissipated into heat or reflected back by area discontinuities. However, no practical muffler or silencer is completely reactive or completely dissipative. Every muffler contains some elements with impedance mismatch and some with acoustic dissipation. Active mufflers, implement noise reduction by creating antinoise of the

same amplitude but opposite phase to the original noise, and they are effective at low frequency [1,2].

The study of acoustical sound propagation in ducts and mufflers is possible by several means. Experimental acoustical study is not often feasible, whereas analytical or numerical methods can often be considered. An introduction to one dimensional duct acoustic modeling can be found in Munjal [3]. Four-pole transfer matrix method that is based on plane wave theory offers an approximative way to make a one-dimensional model of muffler acoustics. This approach has been used for transmission loss optimization in duct system in Yeh et.al. [4]. However, the method is limited to simple geometries and boundary conditions.

Design procedures for resonator mufflers are also given in Beranek [5] and Bies and Hansen [6], but the process is complex. The procedure is used to specify the resonant frequency of the muffler and the desired attenuation. A cavity volume is calculated and then the area of the openings (or connectors) between the exhaust pipe and the cavity must be calculated. Finally a wire or cloth screen to cover the openings must be chosen with the correct flow resistance to provide the correct damping (this reduces the maximum attenuation, but helps to reduce the effect of the pass bands where no insertion loss is achieved when half the acoustic wavelength equals the cavity length). Their performance also deteriorates at higher frequencies when the cross axis dimension of the muffler is 82% of the acoustic wavelength. Due to the legislation rules, the need to introduce new non-fibrous materials is becoming more and more important.

MPP absorbers have the potential to be used instead of porous materials in dissipative mufflers, which not only offers a non-fibrous alternative but also can save weight. This helps to avoid the harmful effects of some fibrous materials on health, especially when they are applied in heating, ventilation and air-conditioning (HVAC) systems. The fundamental design of MPPs was developed by Maa in the nineteen seventies and is currently used for the acoustic conditioning of rooms [7,8,9]. Nevertheless, in industry, this application is still in development. Generally, the micro perforated sheet is characterized by its acoustic impedance. When the acoustic wave spreads across the micro perforations, whose dimensions are in the same order of magnitude of the thermal and viscous boundary layers, a part of the acoustic energy is transformed by friction and heat exchange [10,11,12,13]. Coupled the MPP with a rigid wall by an air space, such a system is similar to an improved Helmholtz resonator. To obtain an absorbing system with a larger frequency range than a classical Helmholtz resonator, the perforation diameter must be sub-millimeter. It leads to a system more efficient in situations of high mechanical or thermal strain, in comparison with flexible porous material.

Moreover, the users' demand for a more compact muffler design as a prerequisite inside a limited-space working area is widely prevalent which is rarely tackled. In previous papers, the shape optimizations of simple-expansion mufflers were discussed [14,15,16,17].

To optimize the sound transmission loss of real mufflers under space constraints, it can be achieved by choosing the best design of muffler and using an efficient sound absorber [18,19,20]. In order to make quick muffler designs and predict its performance which can help the designer to come up with an optimum design, there are many available methods such as Finite Element Method (FEM), Boundary Element Method (BEM), and the most popular one is the Transfer Matrix Method (TMM). In this paper, the effect of using MPP as another alternative to improve the acoustic performance of a muffler is discussed. Based on 1-D program, TMM is used for choosing the muffler shape optimum dimensions and the appropriate MPP absorber while the FEM is used to calculate the muffler final TL results for 3-D effects purposes. This paper represents an attempt to contribute in both categories by optimizing the muffler dimensions and choosing an efficient sound absorber to achieve the highest transmission loss.

1.2. Structure of the Paper

Theoretical models for sound transmission loss in MPP muffler is firstly derived and used to study the effect of internal design of its acoustic performance. The model is based on the wave propagation in two coupled pipes through MPP. The MPP impedance, which is used in the calculation is summarized. The Theoretical model is validated using the measured results. The muffler shape and its internal design configuration are optimized to achieve the maximum transmission loss are presented. The effect of the optimized muffler on the acoustic performance of diesel engine is presented. Comparison between the measured Sound Pressure Level (SPL) and Brake specific fuel consumption (B.s.f.c.) for optimized muffler and the existing one with a straight pipe is introduced.

2. Design of Disipative Muffler

2.1. General

Typical muffler design is shown in Figure 1. This design is chosen because of its low cost and it causes low pressure loss. From an acoustic stand point the muffler has multiple cavities that are connected to the exhaust pipe by the holes illustrated on the central tube.

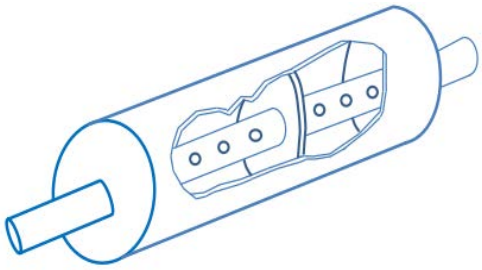

Figure 1. Sketch of a dissipative muffler

In general, for a dynamic muffler consisting of n elements the transfer matrix relation for this can be written by successive application of definition.

$$\begin{pmatrix} p_o \\ q_o \end{pmatrix} = [T_1][T_2].....[T_r].....[T_n][T_{n+1}]\begin{pmatrix} p_{n+1} \\ q_{n+1} \end{pmatrix} \quad (1)$$

where, the transfer matrix is defined as

$$[T_n] = \begin{bmatrix} T_{11} & T_{12} \\ T_{21} & T_{22} \end{bmatrix}_n \quad (2)$$

In this way, the overall transfer matrix can be found out for cascaded one-dimensional systems such as acoustic filters or mufflers. Once it is obtained, the performance can be easily calculated from the four-pole parameters. There is no limit to the maximum number of elements that can be used in the above transfer matrix approach.

2.2. Computing the Transfer Matrix

With the reference to Figure 2 and based on an earlier published paper by Allam and Åbom [10,21], the governing Equations for 1D acoustic waves in this system are

$$\frac{\partial \rho_j}{\partial t}+U_{oj}\frac{\partial \rho_j}{\partial x}+\rho_{oj}\frac{\partial u_j}{\partial x}=(-1)^j\frac{4\rho_w}{d_j}u_w, \tag{3}$$

and

$$\rho_{oj}\left(\frac{\partial}{\partial t}+U_{oj}\frac{\partial}{\partial x}\right)u_j=-\frac{\partial p_j}{\partial x}. \tag{4}$$

and

$$Z=(p_1-p_2)/u_w. \tag{5}$$

Here $j=1,2$ denotes the inner pipe and outer chamber, ρ is density (mean with subscript o), p acoustic pressure, U_o mean flow speed and u acoustic velocity. The coupling between the fields in the inner pipe and outer chamber 1 and 2 is done via acoustic impedance.

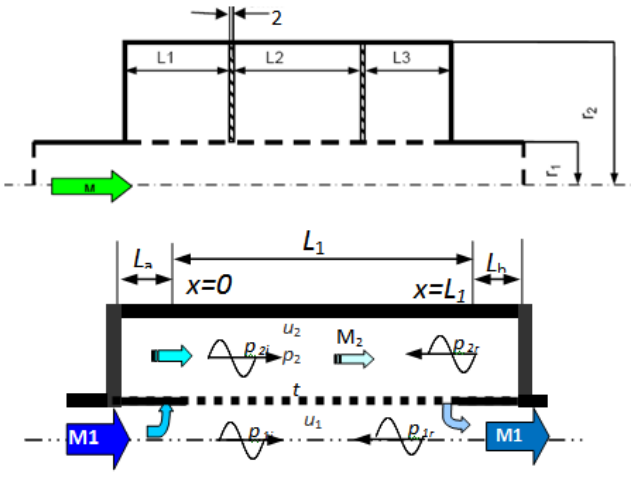

Figure 2. Flow distribution and the acoustic waves in the test object

To solve the problem, a propagating wave ansatz is made and harmonic space and time dependence are introduced. Suppressing the harmonic time dependence ($e^{i\omega t}$) the fluctuating quantities can then be written as

$$\begin{aligned} p_j(x)&=\hat{p}_j\,e^{-iKx},\\ u_j(x)&=\hat{u}_j\,e^{-iKx},\\ \hat{p}_j&=c_j^2\,\hat{\rho}_j,\ \hat{p}_j=Z_j\hat{u}_j \end{aligned} \tag{6}$$

Substituting Equations 5 and 6 into Equation (2) gives

$$\rho_{0j}\left(i\omega+U_{0j}(-iK)\right)Z_j^{-1}=iK. \tag{7}$$

Using Equation 7, the characteristic wave impedance can be obtained

$$Z_j=\frac{\rho_{0j}\omega-\rho_{0j}U_{0j}K}{K}=\frac{\rho_{0j}c_j\left(k_j-M_jK\right)}{K}, \tag{8}$$

where $M_j=U_{0j}/c_j$, and $k_j=\omega/c_j$. Substituting Equations 5 and 6 into Equation 1 and with the help of Equation 8 gives

$$\begin{aligned} &\left(\frac{ik_j}{c_j}\right)\hat{p}_j-\left(\frac{iM_jK}{c_j}\right)\hat{p}_j-\frac{iK^2}{c_j\left(k_j'-M_jK\right)}\hat{p}_j\\ &=(-1)^j\frac{4\rho_w}{D_jZ}(\hat{p}_1-\hat{p}_2). \end{aligned} \tag{9}$$

This equation is simplified by multiplying with i,c_j , $D_1=d$, $D_2=\left(d_2^2-d_1^2\right)/d_1$ and putting $B_j=\frac{c_j\rho_w}{D_jZ}$, which gives

$$\begin{aligned} &-\left(k_j-M_jK\right)\hat{p}_j+\frac{K^2}{\left(k_j-M_jK\right)}\hat{p}_j\\ &=(-1)^j\,4iB_j(\hat{p}_1-\hat{p}_2). \end{aligned} \tag{10}$$

Equation 10 represents a pair of homogenous linear equations which have non-trivial solutions (eigenvalues) for the wave-numbers K corresponding to free waves in the two channels. This linear equation system can be written as

$$\begin{pmatrix} K_1^2+4iB_1(k_1-M_1K) & -4iB_1(k_1-M_1K)\\ -4iB_2(k_2-M_2K) & K_2^2+4iB_2(k_2-M_2K)\end{pmatrix}\begin{pmatrix}\hat{p}_1\\ \hat{p}_2\end{pmatrix}=\begin{pmatrix}0\\0\end{pmatrix} \tag{11}$$

where $K_j^2=K^2-\left(k_j-M_jK\right)\left(k_j-M_jK\right)$. Equation 11 defines a forth order algebraic equation for the wave-numbers K_n , n =1,2,3,4. To each of the wave-numbers there is a corresponding 2-D mode (eigenvector) $\mathbf{e}_n$. The eigenvalues and corresponding modes can be calculated numerically for instance by using Matlab. Using these eigenvalues and modes a general expression for the sound field can be obtained in the form of a 4x4 matrix H(x), which defines the relationship between p and q (the volume velocity) and the modal amplitudes at a cross-section x. Applying this result to x=0 and x=L and solving the modal amplitudes from the second of these equations and putting the result into the first, the four-port transfer matrix $\mathbf{S}=\mathbf{H}(0)\mathbf{H}^{-1}(L)$) is calculated [10,21].

$$\begin{pmatrix}\hat{p}_1(0)\\ \hat{q}_1(0)\end{pmatrix}=\mathbf{T}_P\begin{pmatrix}\hat{p}_2(L)\\ \hat{q}_2(L)\end{pmatrix}, \tag{12}$$

This four-port matrix is then reduced to a two-port matrix **Tp** by using the rigid wall boundary conditions in pipe 2, the rigid-end boundary in pipe 2 yields [21]

$$\begin{matrix}\hat{q}_2(0)/\hat{p}_0(0)\\ \hat{q}_2(L)/\hat{p}_0(L)\end{matrix}=\begin{cases}-j\tan(k_2L_a)\\ j\tan(k_2L_b)\end{cases}=\begin{cases}X_1\\ X_2\end{cases} \tag{13}$$

Where L_a and L_b are shown in Figure 2(b)

$$T_p(x)=\begin{pmatrix}T_p(1,1) & T_p(1,2)\\ T_p(2,1) & T_p(2,2)\end{pmatrix} \tag{14}$$

Where

$$T_p(1,1)=\frac{\begin{pmatrix}S_{22}X_1S_{11}+S_{12}S_{41}-X_1S_{14}X_2S_{21}\\-S_{11}X_2S_{44}-X_1S_{12}S_{21}-S_{11}S_{42}\\+X_1S_{11}X_2S_{24}+S_{14}X_2S_{41}\end{pmatrix}}{\left(-S_{42}+X_1S_{22}-X_2S_{44}+X_2X_1S_{24}\right)}$$

$$T_p(1,2)=\frac{\begin{pmatrix}S_{12}S_{43}-X_1S_{12}S_{23}-S_{13}X_2S_{44}\\+X_1S_{13}X_2S_{24}-S_{13}S_{42}+S_{14}X_2S_{43}\\+S_{31}S_{42}+S_{31}X_2S_{44}\end{pmatrix}}{\left(-S_{42}+X_1S_{22}-X_2S_{44}+X_2X_1S_{24}\right)}$$

$$T_p(2,1)=\frac{-\begin{pmatrix}-S_{22}X_1S_{31}-S_{34}X_2S_{41}+X_1S_{34}X_2S_{21}\\-X_1S_{31}X_2S_{24}+X_1S_{32}S_{21}-S_{32}S_{41}\\+S_{31}S_{42}+S_{31}X_2S_{44}\end{pmatrix}}{\left(-S_{42}+X_1S_{22}-X_2S_{44}+X_2X_1S_{24}\right)}$$

$$T_p(2,2)=\frac{-\begin{pmatrix}-S_{33}X_2S_{44}-S_{22}X_1S_{33}+X_1S_{34}X_2S_{23}\\-X_1S_{33}X_2S_{24}+S_{33}S_{42}+X_1S_{32}S_{23}\\-S_{32}S_{43}-S_{34}X_2S_{43}\end{pmatrix}}{\left(-S_{42}+X_1S_{22}-X_2S_{44}+X_2X_1S_{24}\right)}$$

Which can simplified as

$$T_p(x)=\begin{pmatrix}S_{11}+A_1A_2 & S_{13}+B_1A_2\\S_{31}+A_1B_2 & S_{33}+B_1B_2\end{pmatrix} \quad (15)$$

$$A_1=\left(X_1S_{21}-S_{41}\right)/F_1,\ A_2=\left(S_{12}+X_2S_{14}\right)$$
$$B_1=\left(X_1S_{23}-S_{43}\right)/F_1,\ B_2=\left(S_{32}+X_2S_{34}\right)$$
$$F_1=S_{42}+X_2S_{44}-X_1\left(S_{22}+X_2S_{24}\right)$$

In case of L_a and L_b are equal to zero, i.e. X_1 and X_2 in Equation 13 will be equal to zero also, the wall boundary conditions in pipe 2 will be $\hat{q}_2(0)=0$ and $\hat{q}_2(L)=0$ [11]. A straightforward derivation using Equation 14 reveals that

$$\mathbf{T}_P(x)=\begin{pmatrix}S_{11}-S_{12}S_{41}/S_{42} & S_{13}-S_{12}S_{43}/S_{42}\\S_{31}-S_{32}S_{41}/S_{42} & S_{33}-S_{32}S_{43}/S_{42}\end{pmatrix} \quad (16)$$

The total transfer matrix can be calculated using Equation 2

$$\mathbf{T}=\mathbf{T}_{PI}\ \mathbf{T}_{PII}\ .....\mathbf{T}_{PN} \quad (17)$$

where N is the number of chambers. Then the transmission loss is calculated using.

$$TL=10\log_{10}\left\{\begin{array}{l}\left(\frac{1+M_{in}}{1+M_{out}}\right)^2\frac{Z_{in}}{4Z_{out}}\\\times\left|T_{11}+\frac{T_{12}}{Z_{out}}+Z_{in}T_{21}+\frac{Z_{in}T_{22}}{Z_{out}}\right|^2\end{array}\right\} \quad (18)$$

where M_{in}, M_{out} and Z_{in}, Z_{out} are the Mach-numbers and the acoustic impedance at the in- and outlet of the pipes.

2.3. Transfer Impedance Equations Including Grazing Flow

The MPP impedance is calculated based on the investigations presented in by the authors in references [10,11,12]. MPP impedance z=r+jx, is the specific impedance Z divided by the characteristic impedance of air ρc, where ρ is density and c speed of sound. The normalized impedance of a perforated plate is z divided by the porosity σ can, for circular holes, be expressed as:

$$r=\mathrm{Re}\left(\frac{j\omega t}{\sigma c}\left(1-\frac{2}{\kappa\sqrt{-j}}\frac{J_1\left(\kappa\sqrt{-j}\right)}{J_0\left(\kappa\sqrt{-j}\right)}\right)^{-1}\right) \quad (19)$$
$$+\frac{2\alpha R_s}{\sigma\rho c}+\frac{\left|\hat{u}_h\right|}{\sigma c}+K\,M_g/\sigma$$

and

$$x=\mathrm{Im}\left(\frac{j\omega t}{\sigma c}\left(1-\frac{2}{\kappa\sqrt{-j}}\frac{J_1\left(\kappa\sqrt{-j}\right)}{J_0\left(\kappa\sqrt{-j}\right)}\right)^{-1}\right) \quad (20)$$
$$+\frac{\delta\omega F_\delta\left(1+\frac{\left|\hat{u}_h\right|}{\sigma c}\right)^{-1}}{\sigma c}$$

where ω is the angular frequency, $\kappa=d\sqrt{\omega/4\nu}$ is a dimensionless shear wave number relating the hole radius to the viscous boundary layer thickness, ν is the kinematic viscosity, J_0 and J_1 are the Bessel function of the first kind of zero and first order respectively, determined this end correction δ which equals 8d/3π, α is a factor which equals 4 for sharp edges and (based on our measured data) equals 2 for holes with rounded edges, $R_s=\frac{1}{2}\sqrt{2\eta\rho\omega}$, where η is the dynamic viscosity, $\left|\hat{u}_h\right|$ is the absolute value or the peak particle velocity inside the holes, t is the MPP wall thickness, M_g is the grazing flow Mach number and $F_\delta=\left(1+\left(12.6\cdot M_g\right)^3\right)^{-1}$ represents the flow effect on reactance and K=0.15+/- 0.0125 (std).

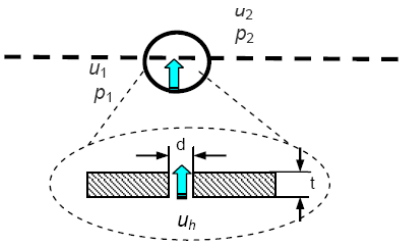

Figure 3. Schematic of a MPP and definition of thickness (t) and diameter/width (d)

2.4. Model Validation

Based on the measured results for the three equal chamber muffler without mean flow [11] which are represented in Figure 4, one can find the minima in the transmission loss occurs when the chamber length equals a multiple of half a wavelength. It can be also noted that it is modified when the chamber lengths are unequal. The last type of configuration therefore provides some advantages without significant reductions of the TL at other frequencies. Through the transmission loss calculation, the nonlinear effect is not included in the MPP impedance formulas for simplicity. That probably explains why one

can find a shift between the measured and predicted results at low frequencies as seen in Figure 4. This configuration also gives the motivation to seek the optimum performance of such muffler.

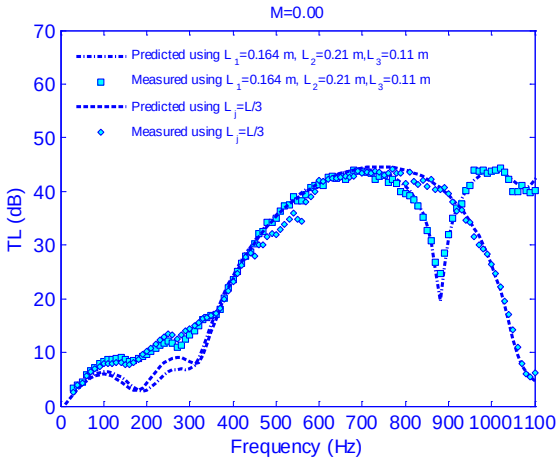

Figure 4. Simulated and measured transmission loss versus frequency for 3 MPP chambers muffler. r1=28.5, r2=75 mm [10]

3. Muffler Shape Optimization

3.1. Acoustic Based Method

Generally, to avoid any minima for certain range of frequencies the chamber length must be less than half sound wave length; i.e. $L_{ch} \langle \lambda/2 \langle c/2f$ which means that $f_{\max} \langle c/2L_{ch}$ with

$$L = n L_{ch} + (n-1)t \qquad (21)$$

where, L is defined as the total available length and ***n*** is the number of chambers. To avoid the deterioration in the transmission loss the chamber length $L_{ch} \le 0.9c/2f_{\max}$ can be used. So to build a muffler without minima in range of frequencies up to 1500 Hz at the cold condition $L_{ch} \le 0.9c/(2f_{\max}) \le 0.102$ and for the case under investigation the chamber length can be $L_{ch} = 0.0992$ m i.e. the total muffler is divided into 5 chambers. For the hot condition at exhaust temperature (800 °K) with c=565 m/s $L_{ch} = 0.166$ m and the muffler is divided into three chambers. The results of both cases are presented in Figure 5. Based on that results, one can notice that even if the chamber length is equal to 90% of the wave length, the acoustic performance also deteriorates at higher frequencies and to avoid that, the cross axis dimension of the muffler must be 82% of the acoustic wavelength, i.e. the chamber length in the cold condition can be $L_{ch} \le 0.093$, and the total length can be divided into six chambers. Also, in hot condition, the chamber length should be $L_{ch} \le 0.153$ m i.e. the muffler is divided into four chambers. The effect of MPP wall on the acoustic performance of 4 chambers Muffler is presented in Figure 6. Figure 7 represents the surface pressure of 4 chambers muffler with and without MPP, which is performed using Comsol multiphysics [22]. Based on the results in Figure 6, the MPP not only provides an enormous achievement in transmission loss (in middle frequency rang) but also prevents the whistling generation due to shape edge of the inner walls.

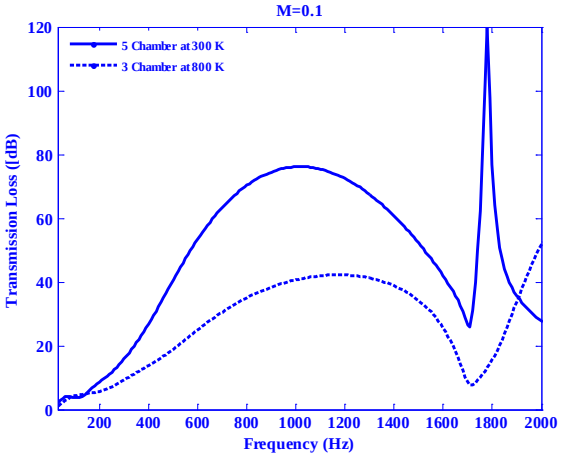

Figure 5. Transmission loss versus frequency for 3 and 5 chambers muffler

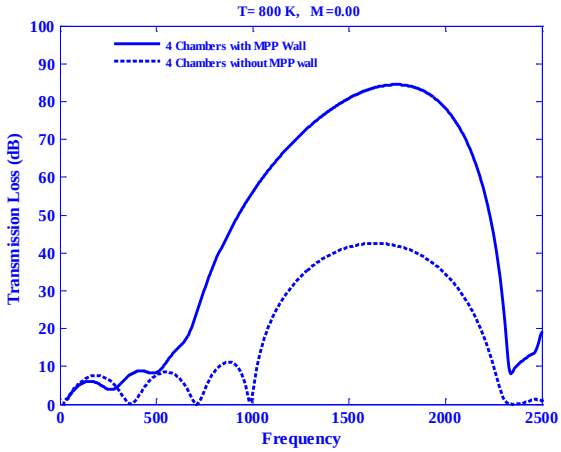

Figure 6. Transmission loss versus frequency of 4 chambers muffle with and without MPP at M=0 and T=800˚K

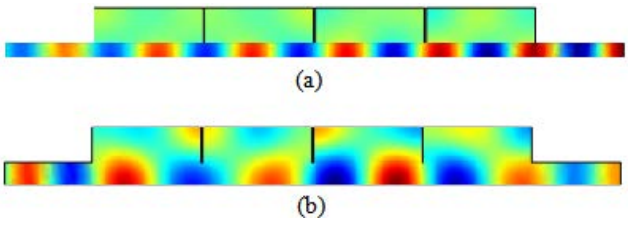

Figure 7. Surface pressure of 4 chambers muffle a) with MPP wall and without MPP wall at 3500 Hz, M=0, T=800˚K. The highest pressure represented by red color, while the blue represents the low pressure

3.2. Numrical Based Method

Numerically, to maximize the transmission loss value (TL), the minimal value of - $f(X)$ is planned and proceeded [18,19]. Minimize $F(X)$ = - $f(X)$ is the Objective function, where $F(X) = TL(X_1, X_2, .., X_j)$, where $X^T = [X_1\ X_2\ ..\ X_j]$ are design variables (length of chambers) and based on Figure 2 and Figure 6(a), j=12. Shape constrains are $X_1 + X_2 + ... + X_n = 0.5 - (n-1)t$ and $g_j(X) \le 0$, j = 1, 2,.., n inequality constraints $L_{chj} \le 0.9c/f_{\max}$.

The solution of the problem has been done using constrained nonlinear multivariable optimization in Matlab[11], where the initial design data is $X_o^T = [0.001\ 0.001\ .....0.001]$. In order to minimize the most objectionable noise components, the objective function was chosen as the average transmission loss over a frequency range of 15-1500 Hz. This range was selected to minimize the noise transmission of at all engine speed from 900 rpm. The transmission loss was evaluated, by using plane wave analysis, at increments of 5 Hz over that range. The resulting objective function is therefore

$$TL(f) = \frac{1}{N}\sum_{1}^{N} TL(f) \tag{22}$$

where, f is the frequency (Hz) and N is the number of frequencies. For the accuracy purpose in plane wave theory, the shape constraint of a long chamber is required. The numerical results for the best dimensions are shown in Figure 8, while the results for the acoustic based method is given in Figure 9.

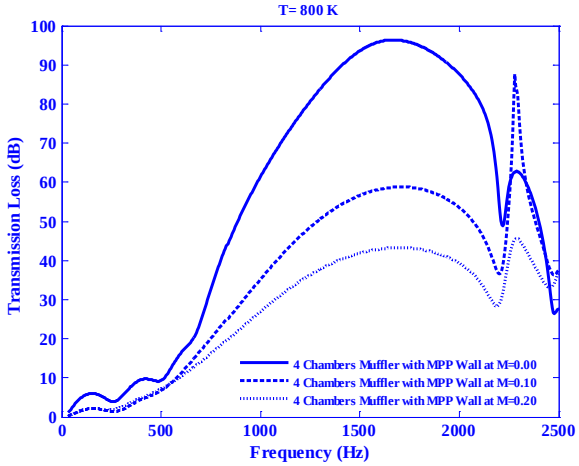

Figure 8. Transmission loss versus frequency at M = (0 – 0.2), c=565 m/s, T=800 ˚K, t=1mm, dh=1mm, σ=2%, r1=28.5 mm, and r2=75 mm at L=[23.9 105.9 00 00 115.9 00 00 115.5 00 00 105.6 25.1]mm

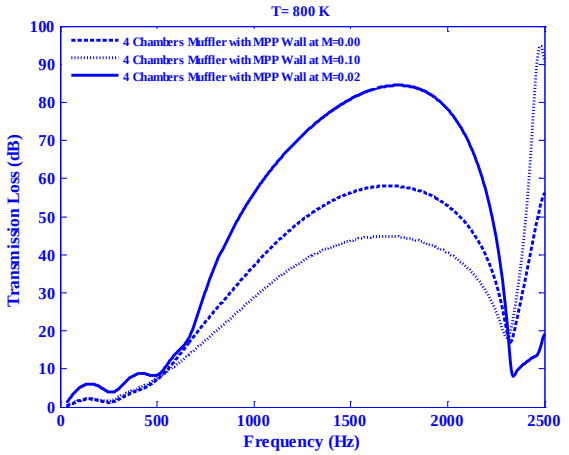

Figure 9. Transmission loss versus frequency at M = (0 – 0.2), c=565 m/s, T=800 ˚K at L2= L5= L8= L11 =123 mm, t=1mm, dh=1mm, σ=2%, r1=28.5 mm, and r2=75 mm

As can be seen from results presented in Figure 8 and Figure 9, when the exhaust flow Mach number is increased through the inner pipes, the sound transmission loss is decreased. This is due to a vortical flow is created in each hole, which connecting the inner pipe to the cavity. This has a significant effect on the connectivity between the two domains (inner and outer pipes) and reducing the transmission loss.

3.3. Wall Maximum Damping Achievement

With the reference to Figure 2 and in the limit of a large number of outer chambers and a local reaction the wall impedance is given by:

$$Z_{Wall} = Z_{MPP} + Z_{cavity} \tag{23}$$

where

$$Z_{cavity} = \frac{i\left(H_0^{(1)}(kr) - \dfrac{H_1^{(1)}(kR)}{H_1^{(2)}(kR)} H_0^{(2)}(kr)\right)}{H_1^{(1)}(kr) - \dfrac{H_1^{(1)}(kR)}{H_1^{(2)}(kR)} H_1^{(2)}(kr)}, \tag{24}$$

Here H denotes Hankel functions of the (1):st and (2):nd kind and orders 0 and 1, r is the cavity inner radius and R denotes the outer radius of the cavity.

The cavity impedance will vary between a stiffness and inertia character, which means there exists (resonance) frequencies at $\mathrm{Im}(Z_{wall}) = 0$. For resonator (side-branch) type of silencers, this is the frequency where the largest transmission loss occurs. Also for the MPP silencer that was studied here the transmission loss at this resonant condition should be an interesting measure, related to the "maximum" damping.

To get the best wall performance for the entire frequency range of interest, the imaginary part of the wall impedance must be minimized, minimize $F(X) = \mathrm{Im}(Z_{Wall})$, object function, subject to $1^{-4} \le h \le 0.07$, where h is the cavity depth (difference between out radius and inner radius), the hole diameter d is 1 mm, the wall thickness t is 1 mm and the wall porosity σ is 2 percent. Based on the numerical optimization, the best cavity depth is 48.8 mm. Based on the results in Figure 10, the bigger volume improves the low frequency damping.

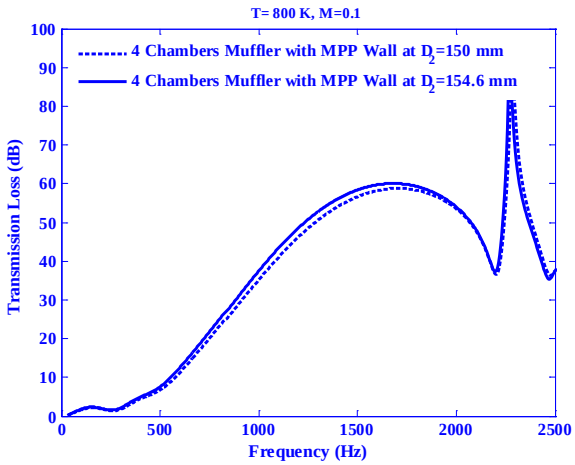

Figure 10. Effect of Flow on Sound Transmission loss of optimized 4 chambers muffler. t=1mm, dh =1mm, σ=2%, r1=28.5 mm, r2=77.6 mm and L= [23.9 105.9 00 00 115.9 00 00 115.5 00 00 105.6 25.1]mm

Another idea to optimize the damping is to match this wall impedance with the Cremer impedance [23] at one frequency. The latter was derived to obtain the highest sound damping in an infinite channel. The concept was developed further by Tester in [24,25], who derived the expression for the circular cross-section, and also added the plug-flow correction as follows:

$$Z_{Cremer} = \frac{(0.88 - j0.38)}{(1+M)^2}\frac{kr}{\pi} \quad (25)$$

The idea is to optimize the damping to match this wall impedance given in Equation 23 with the Cremer impedance given by Equation 25, i.e.,

$$Z_{Cremer}\big|_{Opt} = Z_{MPP} + Z_{cavity} \quad (26)$$

Assume we chose this matching frequency to half the cut-on which for a circular duct is: $kr = 1.84$, using a duct diameter of 57 mm (typical for automotive) gives a cut-on (c=343 m/s) of 1760 Hz and based on [26], it reduces to 1450 Hz at M=0.1 and to 1220 at M=0.2.

Based on the results in Figure 11, using Equation 25 and 26, the cavity depth can be calculated as;

$$Z_{cavity} = -0.79\,j \quad (27)$$

Using Equation 24 with Equation 27, the cavity depth can be calculated numerically and it gives h=40.5 mm.

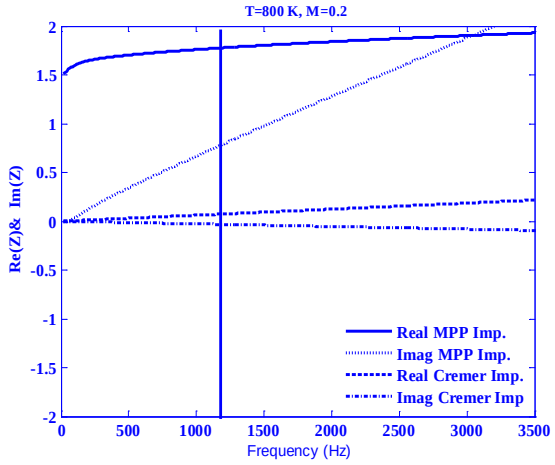

Figure 11. Comparison between MPP and Cremer impedance at real working condition

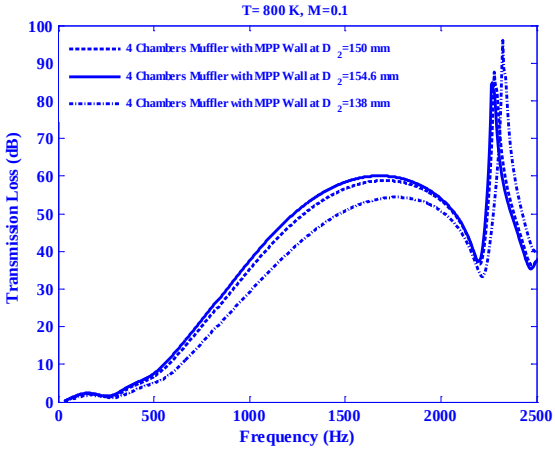

Figure 12. Effect of Flow on Sound Transmission loss of optimized 4 chambers muffler at, r1=28.5 mm, and r2=77.6 mm

Using the calculated cavity death, the sound transition loss is calculated and compared with such results presented in Figure 10 and presented in Figure 12, which shows the sound transmission loss can be improved at resonant frequency at smaller diameter, while the bigger diameter improves the muffler performance at low frequency, which is important for automotive application because the pulse is repeated at the firing frequency of the engine. So, it is decided to use the optimized dimensions, which are listed under Figure 10.

4. Effect of New Developed Muffler on Diesel Engine Acoustic Performance

4.1. General

The Transmission Loss, noise reduction, Insertion Loss and radiated noise are the major characteristics used to describe the performance of a muffler in an automotive exhaust system. Out of these characteristics, Insertion loss and exhaust radiated sound pressure levels play a significant role in muffler design as they are a measure of true performance of muffler along with engine/vehicle and very much useful for the designers to compare different silencer configurations. In the present work, the radiated noise is measured by the ISO 3745 and the background noise is 40 dB lower than the measured sound pressure level from the source under test in each frequency band.

4.2. Experemental Set-up

The block diagram of the set-up is shown in Figure 13. The diagram is self-explanatory. The experiments were conducted in the Internal Combustion Engines Laboratory of the Automotive Technology Department at Faculty of Industrial Education, Helwan University, Cairo, Egypt. All noise data was taken on a relative basis in the closed space of the laboratory and in the presence of other equipment, engines and instruments in the close vicinity of the muffler exit and nearest wall was at 6 m away. The background noise was recorded before experimentation. In order to keep background noise to a minimum, all other engines and machines in the laboratory were shut down during recording of the background noise. The engine was mounted on a test cell.

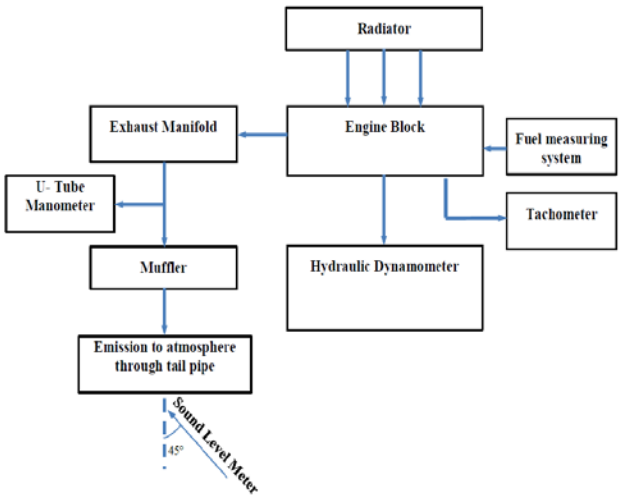

Figure 13. Sketch of the experimental set-up

In order to carry out the related experiments, the RO-line precision sound level meter type 1350 is used. It is a precision-class instrument with digital display, measuring maximum r.m.s. sound pressure level and easy to use. The type 1350 meter has a built-in A-weighting and 'fast' and 'slow' r.m.s. detector characteristics. It fulfills the IEC type 1, DIN IEC 651 type 1 and ANSIS 1.4 1983 type S1-A requirements [27,28,29]. The sound level meter was placed at an angle of 45° to the center-line of the tail pipe of the muffler, at a distance of 1 m from the tail pipe exit.

The engine speed and torque were set to the appropriate values simultaneously. Data was taken for speeds of 1000, 1500, 2000, 2500 and 3000 r/min and loads of 0, 40, 80, 120, 160 and 200 N m corresponding to each r/min.

The back pressure across the muffler was determined with the help of an inclined U-tube manometer. The hydraulic dynamometer was used to determine the developed torque. A load cell was used to pick up the torque signals, which were fed to a digital torque meter for readout**.** An electromagnetic pickup between the Gardner shaft of the engine and the dynamometer shaft was used to determine the engine r/min.

4.3. Assumptions

1. Variations in ambient temperature do not affect the reading to a large extent.
2. The engine noise remains the same for a particular load and r/min irrespective of the muffler at the engine exhaust.
3. The recorded noise was due to the engine exhaust, mechanical vibration of the engine parts and also echoes resounding from the walls of the laboratory. Under the same conditions of engine r/min and load, the noise due to mechanical vibration of the engine parts and due to the dynamometer remains constant. Hence, any decrease in the recorded noise is due to a decrease in the exhaust noise only.

5. Result and Discussion

During the real engine measurement, the optimized muffler presented in the previous section is used and compared with an existing muffler; which is straight through resonator (hole diameter 5 mm, wall thickness 4 mm, 12% wall porosity, inner pipe diameter 57 mm, outer diameter 150 mm and length is 500 mm) and straight pipe with the same length.

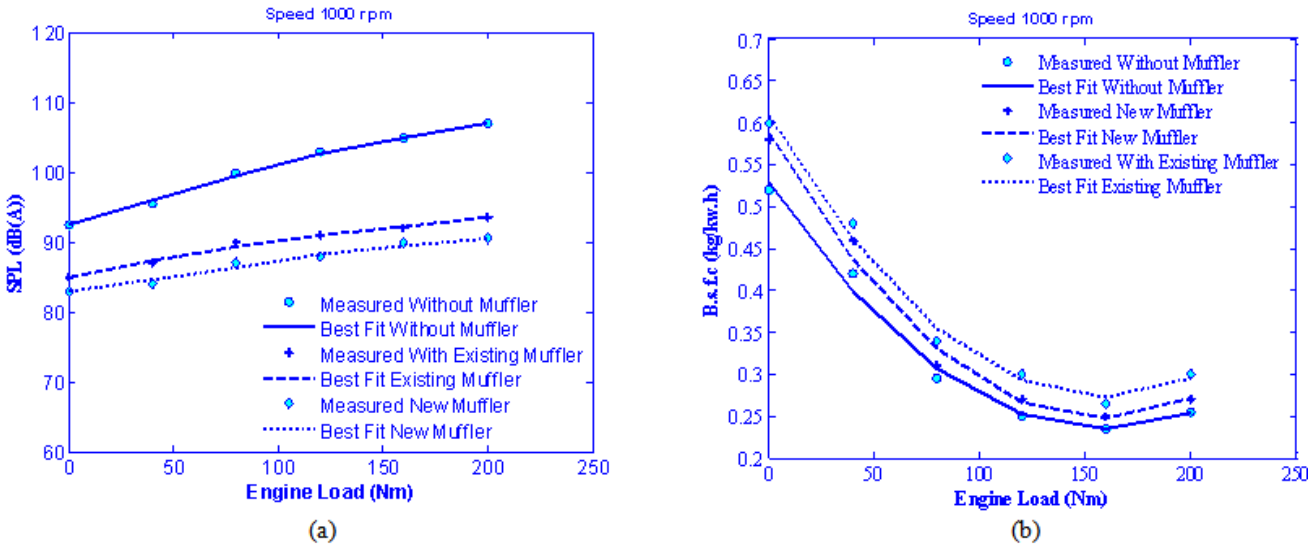

Figure 14. (a) Sound pressure level, (b) brake specific fuel consumption versus load at 1000 r/min

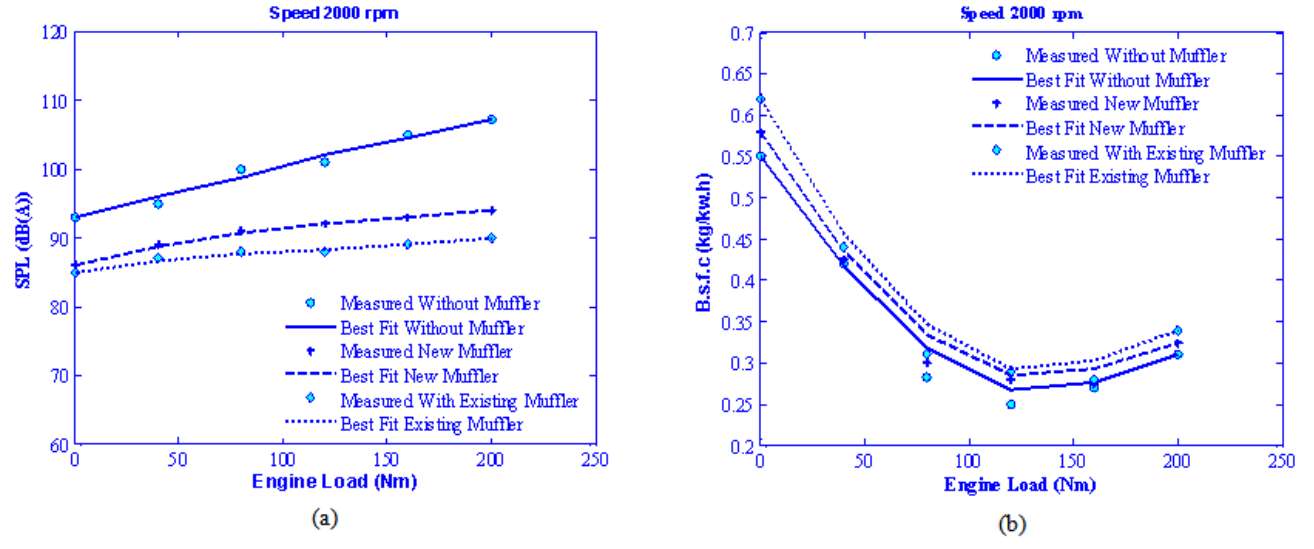

Figure 15. (a) Sound pressure level, (b) brake specific fuel consumption versus load at 2000 r/min

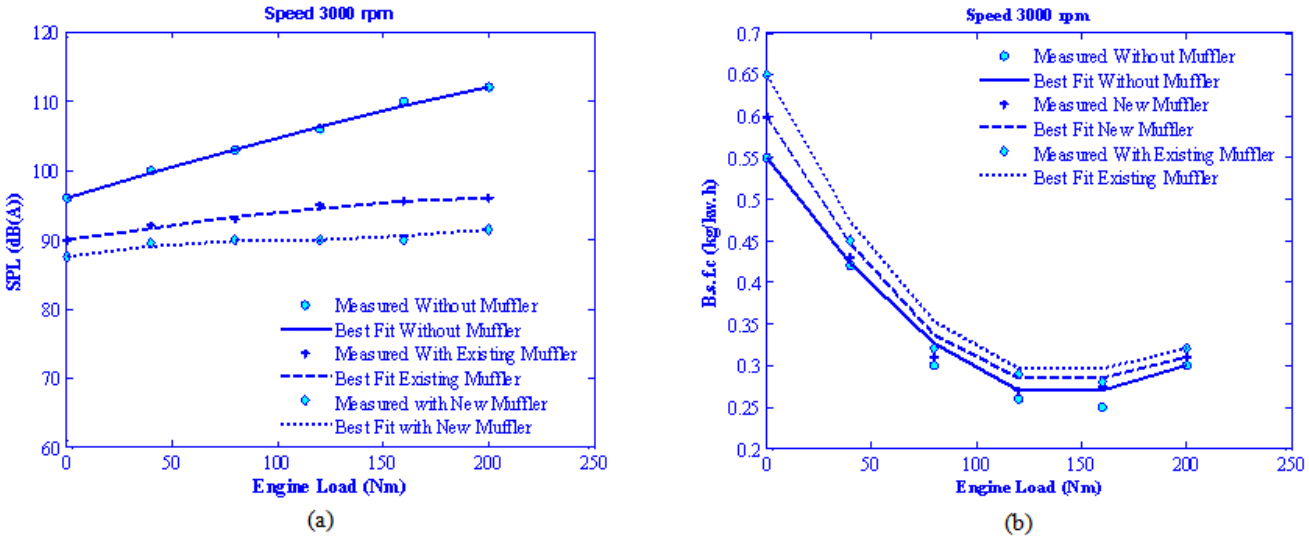

Figure 16. (a) Sound pressure level, (b) brake specific fuel consumption versus load at 2000 r/min

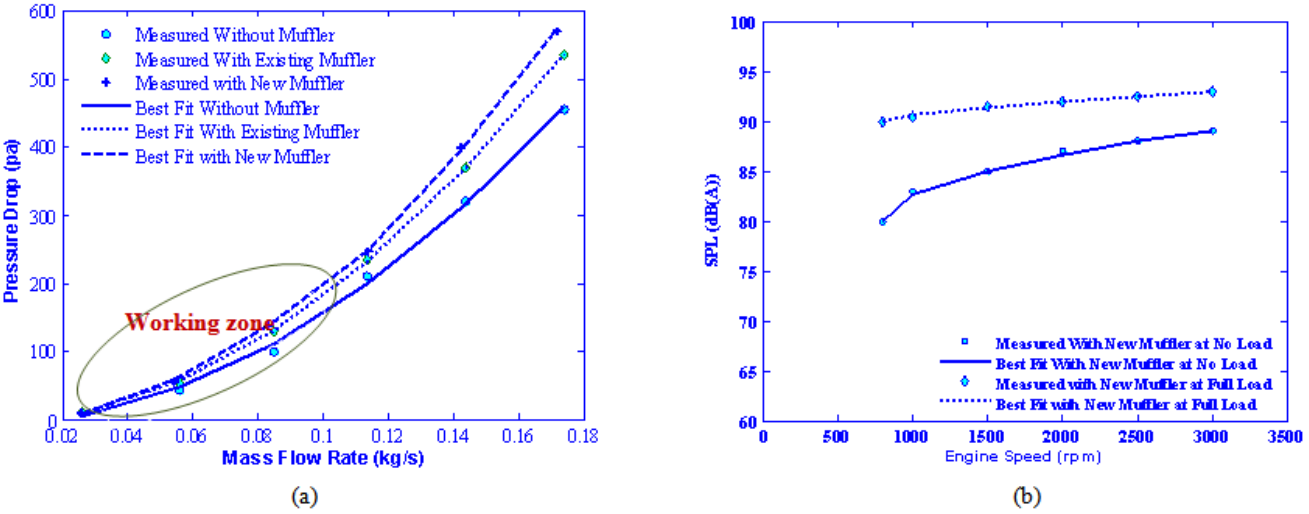

Figure 17. (a) Pressure drop versus Mass flow rate, (b) Sound pressure level versus engine speed

Figure 14 to Figure 17 represent the measured sound pressure level, brake specific fuel consumption (B.s.f.c) versus load at 1000, 2000, and 3000 r/min respectively. The graphs demonstrate that the new optimized muffler decreases the sound pressure level under all engine conditions. This is due to the configuration having restorative and reactive structures.

The observations show that at no load, for each r/min, there is an increase in back pressure and hence an expected rise in fuel consumption for all test configurations. But as soon as the engine is loaded externally, the back pressure decreases and hence the fuel consumption decreases, and brake specific fuel consumption falls.

The plots of SPL versus load at constant r/min show an increase in noise reduction with increase in load. This is a very favorable feature, since an engine tends to generate more noise at higher loads than at lower loads. The rate of rise in exhaust noise is less steep and hence the progressive increase in load affects the exhaust noise to a lesser extent than with the introduction of the new muffler.

The acoustic performance of new optimized muffler which is shown in Figure 2 and Figure 7 (a); based on its SPL and B.s.f.c is better than the existing one, it can be also fabricated so as to be easily opened for maintenance and repair.

6. Conclusion and Future Work

In this paper two different procedures to optimize the muffler acoustic performance; the acoustical based and the numerical based methods are presented. Using the same boundary conditions, both procedures lead to the different muffler dimensions.

The optimum dimensions of the dissipative muffler are calculated by maximizing the transmission loss using the Transfer Matrix Method or by minimizing the transmitted sound power after the muffler which; can be performed using the incident sound power and the sound transmission loss.

Two different methods to improve the wall impedance are presented and compared. The first method is mainly based on MPP wall and cavity behind, while the second method is based on Cremer impudence, MPP and the cavity behind and the real operating conditions.

The acoustic performance of the four-cylinder diesel engine (via SPL) is recorded with the developed muffler compared with its existing muffler and straight pipe. It has

been noted that the maximum noise reductions recorded with the developed and existing muffler compared with straight pipe were 21.5 dB(A) and 15.5 dB(A) respectively.

Using the new developed muffler instead of the existing one, the engine noise can be reduced by 6 dB(A) and its brake specific fuel consumption is also improved up to 8 percent.

As a future work, full muffler optimization is needed for further improvement of the diesel engine performance.

Acknowledgments

Part of this work is financed by the Sweden-MENA Research Links (SRL-MENA) contract number 348-2008-6199. Another part has been funded by the European Community under the project FlowAirS. Author would like to thank Prof. Mats Åbom, the Head of MWL, at the Aeronautical and Vehicle Engineering Department, KTH, Stockholm, Sweden for all helps, useful and interesting discussions.

References

[1] J. M. Egana, J. Diaz, J. Vinolas, *Active control of low-frequency broadband air conditioning duct noise*, Noise Control Eng. 51 (5) (2003) 292-299.

[2] H. J. Lee, Y. C. Park, C. Lee, D. H. Youn, *Fast active noise control algorithm for car exhaust noise control*, Electron. Lett. 36 (14) (2000) 1250-1251.

[3] M. L. Munjal, *Acoustics of ducts and mufflers*, Chichester: John Wiley, 1987.

[4] L. J. Yeh, Y.-C. Chang, M.-C. Chiu, *Shape optimal design on double-chamber mufflers using simulated annealing and a genetic algorithm*, Turkish J. Eng. Env. Sci. 29 (2005) 207-224.

[5] Ver, I.L., Beranek, L.L, *Noise and vibration control engineering, Second Edition*, John Wiley&Sons, Inc., 2006.

[6] David A. Bies and Colin H. Hansen "*Engineering Noise Control - Theory and Practice*" 2003, Spon Press 11 New Fetter Lane, London EC4P 4EE.

[7] D.-Y, Maa. *Potential of microperforated panel absorber*, Journal of Acoustical Society of America, Vol.104, no.5, July 1998.

[8] D.-Y, Maa, "Theory and design of micro perforated-panel sound-absorbing construction" *Sci. Sin*. XVIII, 55-71 (1975).

[9] D-Y, Maa "Microperforated panel at high sound intensity" *Proc. internoise 94 (Yokohama,1994).*

[10] Allam S. and Abom M., 2011, ''A New Type of Muffler Based on Micro perforated Tubes''. Journal of Vibration and Acoustics'', ASME Journal of Vibration and Acoustics, 133.

[11] Allam, S., and Åbom, M., 2008, "*Experimental Characterization of Acoustic Liners With Extended Reaction*," The 14th AIAA/CEAS Conference 2008, p. 3074.

[12] Guo, Y., Allam, S., and Åbom, M., 2008, "*Micro-Perforated Plates for Vehicle Application*," The 37th International Congress and Exposition on Noise Con- trol Engineering, INTER-NOISE 2008, Shanghai, China, Oct. 26-29.

[13] J. Liu, D. W. Herrin and A. F. Seybert "*Application of Micro-Perforated Panels to Attenuate Noise in a Duct"* SAE 2007-01-2196.

[14] Chang, Y. C., Yeh, L. J., and Chiu, M. C., "*Numerical studies on constrained venting system with side inlet/outlet mufflers by GA optimization*," Acta Acustica united with Acustica, Vol. 90, No. 1-1, pp. 1-11 (2004).

[15] Chang, Y. C., Yeh, L. J., and Chiu, M. C., "*Shape optimization on double- chamber mufflers using genetic algorithm,"* Proceedings ImechE Part C: Journal of Mechanical Engineering Science, Vol. 10, pp. 31-42 (2005).

[16] Yeh, L. J., Chang, Y. C., and Chiu, M. C., "*Numerical studies on constrained venting system with reactive mufflers by GA optimization*," International Journal for Numerical Methods in Engineering, Vol. 65, pp. 1165-1185 (2006).

[17] Min-Chie Chiu "*SHAPE OPTIMIZATION OF ONE-CHAMBER MUFFLERS WITH REVERSE-FLOW DUCTS USING A GENETIC ALGORITHM*", Journal of Marine Science and Technology, Vol. 18, No. 1, pp. 12-23 (2010).

[18] Sabry Allam "*Shape Optimization of Reactive Muffler and Its Effect on I.C. Engine Acous-tic Performance*" The 16th ICSV 2009 - July 5-9, Krakow, Poland.

[19] Sabry Allam "*Shape Optimization of Complex Multi-Chamber Muffler*" The 17th ICSV 2010 - July 17-21, Cairo, Egypt.

[20] Patidar, A., Prasad, S., Gupta, U., and Subbarao, M., "*Commercial Vehicles Muffler Volume Optimization using CFD Simulation*," SAE Technical Paper 2014-01-2440, 2014.

[21] Allam, S., and Åbom, M., 2005, "*Acoustic Modelling and Testing of Diesel Particulate Filters*," J. Sound Vib., 288, pp. 255-273.

[22] *COMSOL Multiphysics 3.5*, User's Guide Copyright 1994-2010.

[23] L. Cremer, "*Theory regarding the attenuation of sound transmitted by air in a rectangular duct with an absorbing wall, and the maximum attenuation constant produced during this process*." 1953 Acustica 3, 249-263. (In German.).

[24] B. J. Tester, "*The Optimization of Modal Sound Attenuation in Ducts, in the Absence of Mean Flow,"* Journal of Sound and Vibration , 1973, 27(4), 477-513.

[25] B.J.Tester, "*The propagation and attenuation of sound in lined ducts containing uniform or "plug" flow*, Journal of Sound and Vibration, 1973, 28(2), 151-203.

[26] M. Åbom, "*Measurement of the scattering matrix of acoustical two-ports*," Journal of Mechanical System and Signal Processing 5 (1991) 89-104.

[27] Lief, N. "*International standards for acoustics and noise control*." J. Noise Control Engng, March–April 1989, 32(2), 67-72.

[28] International Standard IEC 651:1979 Sound Le_el Meters, 1979 (International Electrotechnical Commission, Geneva, Switzerland).

[29] ANSI SI. 1-1994 "*American National Standard Acoustical Terminology*, 1994 (American National Standards Institute, Acoustical Society of America, New York).

Appendix A

Engine specifications

Type	Ford XLD 418
Capacity	1753 mm^3
Injection sequence	1-3-4-2
Bore	82.5 mm
Stroke	82.0 mm
Compression ratio	21.5:1
Exhaust valve open	57° BBDC
Exhaust valve close	7° ATDC
Inlet valve open	6° BTDC
Inlet valve close	32° ABDC